Propagation of solitons in a randomly perturbed Ablowitz-Ladik chain

J. Garnier*

Centre de Mathématiques Appliquées, Centre National de la Recherche Scientifique, Unité Mixte de Recherche No. 7641, Ecole Polytechnique, 91128 Palaiseau Cedex, France

(Received 12 June 2000; published 24 January 2001)

This paper deals with the transmission of a soliton in a discrete, nonlinear, and random medium. A random lattice nonlinear Schrödinger equation is considered, where the randomness holds in the on-site potential or in the coupling coefficients. We study the interplay of nonlinearity, randomness, and discreteness. We derive effective evolution equations for the soliton parameters by applying a perturbation theory of the inverse scattering transform and limit theorems of stochastic calculus.

DOI: 10.1103/PhysRevE.63.026608 PACS number(s): 42.65.Tg, 05.45.Yv, 42.25.Dd, 63.20.Pw

I. INTRODUCTION

This paper is concerned with the competition between randomness and nonlinearity for wave propagation phenomena in the one-dimensional case. As is well known, in one-dimensional linear media with random inhomogeneities strong localization occurs, which means in particular that the transmitted intensity decays exponentially as a function of the size of the medium [1–3]. On the other hand, in homogeneous nonlinear media, wave packets called solitons can be generated. They propagate without change of form and with constant velocities over very large distances [4]. A great deal of work has been devoted to the transmission of a soliton through a slab of nonlinear and random medium, especially in the case of the one-dimensional nonlinear Schrödinger (NLS) equation with cubic nonlinearity [5]. Kivshar *et al.* [6] obtained results in the case of a random medium consisting of pure point impurities with a very low density which affect only the potential. In such conditions the authors showed that there is a threshold below which the pulses decay quickly. This fact was experimentally observed in Ref. [7]. In Ref. [8] we considered the NLS equation, and assumed that inhomogeneities affect the potential and the nonlinear coefficient. Using the inverse scattering transform, we exhibit several typical behaviors. The mass of the transmitted soliton may tend to zero exponentially (as a function of the size of the slab) or following a power law; or else the soliton may keep its mass, while its velocity decreases at a very slow rate.

In this paper we consider a lattice version of the NLS equation, so as to take into account the discreteness for the study of the stability of solitons. The discreteness appears in various physical frameworks (optical waveguide arrays [9,10], electric circuits [11,12], electron trapping in materials [13], etc.), and may induce very different features compared to the continuum NLS equation [14]. The so-called Ablowitz-Ladik (AL) equation [15] is the integrable discretization of the continuum NLS equation, so it is the relevant equation to consider in order to point out the role of discreteness in the interplay between randomness and nonlinearity for soliton propagation phenomena. One can find in the literature a few papers that deal with this problem [16–18]. All of them apply the collective variable approximation or the averaged Lagrangian approach, where the solution is sought in a solitonlike form with time-dependent parameters. Then this ansatz is substituted into the Lagrangian of the system, so that a finite-dimensional system of ordinary differential equations is obtained for the set of soliton parameters. The most significant drawback of this method is that it neglects radiation effects. The main result is obtained by Scharf and Bishop [16]: they considered a smooth potential on the one hand and an impurity potential on the other hand. They showed that the collective variable approach is efficient when dealing with a slowly varying potential in the sense that it is almost constant at the scale of the soliton width. We shall consider more general types of perturbations, and proceed under a different asymptotic framework. Our main contribution is that we use the inverse scattering transform, so as to take into account both the variations of the soliton parameters and the radiation effects. Both effects and their interplay are important, and cannot be neglected when the correlation length of the potential is of the same order as the soliton width. The interaction of different length scales are an important issue in localization. Thus the relationship of the width of the soliton and the correlation length of the potential will clearly have a fundamental effect on the questions we are trying to answer. We shall consider the influence of small random perturbations, and aim at reporting possible asymptotic behaviors when the amplitudes of the random fluctuations go to zero and the size of the system goes to infinity. We shall put several interesting features into evidence as a result of the discreteness of the lattice.

The paper is organized as follows. Section II is devoted to a short review of the Ablowitz-Ladik equation and the discrete inverse scattering. We introduce exact traveling solutions (soliton solutions) of the integrable system, and we also present basic results that are required for our study. In Sec. III we address the random problem at hand: the interaction of a soliton with a random on-site potential. By applying a modified version of the inverse scattering transform, we study the interaction of the soliton and radiation, and we derive an effective system that governs the evolutions of the soliton parameters. This system is carefully studied in Sec. IV. We compare the theoretical results with full numerical

*FAX: (33) 1 69 33 30 11. Email address: garnier@cmapx.polytechnique.fr

simulations of the AL equation in Sec. V. Finally in Sec. VI we consider an Ablowitz-Ladik chain with random coupling coefficients.

II. HOMOGENEOUS ABLOWITZ-LADIK CHAIN

The integrable discretized version of the continuum NLS equation is the so-called AL equation [19]:

$$iq_{nt}+q_{n+1}+q_{n-1}-2q_n+|q_n|^2(q_{n+1}+q_{n-1})=0. \quad (1)$$

This model can be derived from the Hamiltonian

$$H=-2\sum_n \text{Re}(q_n q_{n+1}^*)+2\sum_n \log(1+|q_n|^2) \quad (2)$$

if we take care to adopt the nonstandard Poisson brackets [20]

$$\{q_m,q_n^*\}=i(1+|q_n|^2)\delta_{mn}, \quad \{q_m,q_n\}=\{q_m^*,q_n^*\}=0, \quad (3)$$

where the star stands for the complex conjugation. This integrable version supports moving nonlinear localized excitations in the form of lattice solitons, so we can study the effects of site-dependent on-site potentials with the known analytic behavior of the unperturbed dynamics. We shall begin by a short review of the inverse scattering transform applied to the AL equation.

A. Direct transform: The scattering problem

The scattering problem associated with the AL equation is the Ablowitz-Ladik spectral problem [15]

$$\begin{pmatrix}1&0\\0&1\end{pmatrix}f_{n+1}(z)+\begin{pmatrix}0&q_n\\-q_n^*&0\end{pmatrix}f_n(z)=\begin{pmatrix}z&0\\0&z^{-1}\end{pmatrix}f_n(z),$$

$$f_n(z)=\begin{pmatrix}f_{1,n}(z)\\f_{2,n}(z)\end{pmatrix}, \quad (4)$$

where $z\in\mathbb{C}$ is the spectral parameter. Let us first assume that $q_n\equiv 0$. In such conditions, there exists no solution in l^2 of Eq. (4) whatever z, which means that the discrete spectrum is empty. The continuous spectrum consists of the unit circle of the complex plane $\mathbb{S}^1$; the associated eigenspace is of dimension 2, and the pair of functions $(\mathbf{e}_1 z^n, \mathbf{e}_2 z^{-n})$ is a base of the eigenspace associated with the parameter z, where

$$\mathbf{e}_1=\begin{pmatrix}1\\0\end{pmatrix}, \quad \mathbf{e}_2=\begin{pmatrix}0\\1\end{pmatrix}. \quad (5)$$

From now on, we assume $q_n\not\equiv 0$.

Continuous spectrum. The so-called Jost functions ϕ and ψ are the eigenfunctions which are associated with the eigenvalue z, and which satisfy the following boundary conditions:

$$\phi_n(z)\simeq \mathbf{e}_1 z^n, \quad n\to-\infty, \quad (6)$$

$$\psi_n(z)\simeq \mathbf{e}_2 z^{-n}, \quad n\to\infty. \quad (7)$$

If q_n decays sufficiently rapidly as $|n|\to\infty$ (more exactly for $q\in l^1$), then $\phi_n(z)z^{-n}$ and $\psi_n(z)z^n$ are well defined for any $z\in\mathbb{S}^1$ and can analytically continued for $|z|>1$. Introducing the involution operator Inv

$$\text{Inv}(f)_n(z)\equiv\overline{f}_n(z)=\begin{pmatrix}f_{2,n}^*(1/z^*)\\-f_{1,n}^*(1/z^*)\end{pmatrix}, \quad (8)$$

the vector $\overline{f}$ associated with a vector f solution of Eq. (4) is also a solution of Eq. (4) for the same eigenvalue z. We thus consider also the eigenvectors $\overline{\phi}$ and $\overline{\psi}$ which can be defined either as the involutions of ϕ and ψ, respectively, or as the eigenfunctions which are associated with the eigenvalue z and which satisfy the following boundary conditions:

$$\overline{\phi}_n(z)\simeq -\mathbf{e}_2 z^{-n}, \quad n\to-\infty, \quad (9)$$

$$\overline{\psi}_n(z)\simeq \mathbf{e}_1 z^n, \quad n\to\infty. \quad (10)$$

$\overline{\phi}_n(z)z^n$ and $\overline{\psi}_n(z)z^{-n}$ are analytic for $|z|<1$. Furthermore the Jost functions $\psi(z)$ and $\overline{\psi}(z)$ are linearly independent because their Wronskian

$$W(\psi_n(z),\overline{\psi}_n(z))\equiv\psi_{1,n}(z)\overline{\psi}_{2,n}(z)-\psi_{2,n}(z)\overline{\psi}_{1,n}(z)$$
$$=-\prod_{m=n}^{\infty}(1+|q_m|^2)^{-1} \quad (11)$$

is nonzero. Therefore, they form a base of the space of the solutions of Eq. (4), so that we have the decompositions

$$\phi_n(z)=a(z)\overline{\psi}_n(z)+b(z)\psi(z), \quad (12)$$

$$\overline{\phi}_n(z)=-\overline{a}(z)\psi_n(z)+\overline{b}(z)\overline{\psi}_n(z), \quad (13)$$

where a and b are the so-called Jost coefficients. If follows from Eqs. (12) and (13) in particular that

$$a(z)=\frac{W(\phi_n(z),\psi_n(z))}{W(\overline{\psi}_n(z),\psi_n(z))}, \quad b(z)=\frac{W(\phi_n(z),\overline{\psi}_n(z))}{W(\overline{\psi}_n(z),\psi_n(z))}. \quad (14)$$

From this definition we can see that a is well defined over $\mathbb{S}^1$, and can be analytically continued in the outside of the unit circle. b is well defined over $\mathbb{S}^1$, but there is no reason to believe that it could be continued out of the circle, except if $(q_n)_n$ is exponentially decaying. Furthermore it can be shown by symmetry arguments that $\overline{a}(z)=a^*(1/z^*)$ and $\overline{b}(z)=b^*(1/z^*)$, a is even in z, and b is odd. Finally, letting $n\to-\infty$ in the Wronskian relation (11) yields that, for any $z\in\mathbb{S}^1$:

$$|a(z)|^2+|b(z)|^2=\prod_{n=-\infty}^{\infty}(1+|q_n|^2). \quad (15)$$

Discrete spectrum. Note that if z_1, $|z_1|>1$ is a zero of a, then the functions $\psi(z_1)$ and $\phi(z_1)$ are linearly dependent, i.e., there exists c_1 such that $\phi_n(z_1)=c_1\psi_n(z_1)$ for any n

$\in \mathbb{Z}$. Accordingly, ϕ and ψ are exponentially decaying as $|n| \to \infty$. Since a is even, the zeros come in $\pm$ pairs. We retain only the zeros with a non-negative real part, and number them from 1 to J. The set of quantities $\{a(z), b(z), z \in \mathbb{S}^1; z_j, c_j, a'(z_j), j=1,\ldots,J\}$ is the scattering data for the spectral problem [Eq. (4)].

B. Time evolutions of the scattering data

The time equations for the scattering data are

$$a(t,z)=a(t_0,z), \quad z \in \mathbb{S}^1, \tag{16}$$

$$b(t,z)=b(t_0,z)\exp(i\omega(z)(t-t_0)), \quad z \in \mathbb{S}^1, \tag{17}$$

$$c_j(t)=c_j(t_0)\exp(i\omega(z_j)(t-t_0)), \quad j=1,\ldots,J, \tag{18}$$

where $\omega(z)=2-z^2-z^{-2}$. Note that $\omega(z)$ is the linear dispersion relation of discrete linear Schrödinger equation. Indeed the linear form of Eq. (1) is $iq_{nt}+q_{n+1}+q_{n_1}-2q_n=0$, whose dispersion relation is obtained by letting $q_n=z^{2n}\exp(-i\omega t)$.

C. Inverse transform

Given the set of scattering data, we define

$$\overline{F}(m)=\frac{1}{4i\pi}\oint_{\gamma_u}\frac{\overline{b}}{\overline{a}}(z)z^{m-1}dz-\sum_{j=1}^{J}\overline{c_j z_j^{m-1}}, \tag{19}$$

where $\overline{z_j}=1/z_j^*$, $\overline{c_j}=c_j^*\overline{z_j^2}/a'(z_j)^*$, and γ_u is the positively oriented unit circle. Then we compute the kernel $\overline{K}$ as the solution of the system:

$$\overline{K}(n,n+2p-1)-2\overline{F}(2n+2p-1)$$
$$+4\sum_{p',p''=1}^{\infty}\overline{K}(n,2n+2p''-1)$$
$$\times\overline{F}^*(2n+2p'+2p''-1)\overline{F}(2n+2p'+2p-1)=0. \tag{20}$$

This equation is the discrete analog of the Gel'fand-Levitan-Marchenko integral equation. They are linear summation equations. In such conditions, it can be proved [19] that

$$q_n=-\overline{K}(n,n+1). \tag{21}$$

D. Conserved quantities

Conserved quantities can be worked out as in any integrable system [21].

Proposition II.1. The total mass

$$N_{tot}:=\sum_n \log(1+|q_n|^2) \tag{22}$$

and the kinetic energy

$$E_{\rm k}:=-2\sum_n \mathrm{Re}(q_n^* q_{n-1}) \tag{23}$$

are two of the infinite number of conserved quantities for the homogeneous Ablowitz-Ladik chain.

The derivation of the set of conserved quantities is based on the expansion of the analytic function $\overline{a}(z)$ as $z\to 0$.

Lemma II.2. The function $\overline{a}(z)$ has an expansion as $z\to 0$,

$$\log\overline{a}(z)\simeq\sum_{j=1}^{\infty}C_j z^{2j}, \tag{24}$$

where C_j are time independent. In particular,

$$C_1=-\sum_n q_n^* q_{n-1}. \tag{25}$$

Proof: The following arguments are taken from Ref. [21]. It can be shown from the scattering problem that

$$\log\overline{a}(z)=\sum_n \log g_n(z^2), \quad |z|\le 1, \tag{26}$$

where g_n satisfies

$$g_{n+1}(g_{n+2}-1)-z^2\frac{q_{n+1}^*}{q_n^*}(g_{n+1}-1)=-z^2 q_{n+1}^* q_n. \tag{27}$$

These equations are established by relating $\overline{a}(z)$ to the eigenfunction $\overline{\phi}$ by $\overline{a}(z)=\lim_{n\to\infty}(-\overline{\phi}_{2,n}z^n)$. As $z\to 0$, $g_n(z^2)$ has the expansion

$$g_n(z^2)=\sum_{j=0}^{\infty}g_n^{(j)}z^{2j}. \tag{28}$$

We then find from Eq. (27) that

$$g_n\simeq 1-z^2 q_{n-1}^* q_{n-2}-z^4 q_{n-1}^* q_{n-3}(1+|q_{n-2}|^2)+\cdots. \tag{29}$$

Thus $\overline{a}(z)$, analytic for $|z|<1$, has expansion (24) as $z\to 0$. Further, C_j are time independent, since $\overline{a}(z)$ is time independent. Setting Eqs. (29) and (24) equal, one obtains the desired result.

It will be necessary below to express the mass and energy in terms of scattering data.

Proposition II.3. Let us define $c(z):=\log[1+(|b|^2/|a|^2)]$ for $z\in\mathbb{S}^1$. The total mass and the kinetic energy can be decomposed into the sums of continuous parts and of discrete parts:

$$N_{tot}=\frac{1}{2i\pi}\oint_{\gamma_u}\frac{c(z)}{z}dz+\sum_{j=1}^{J}\log|\zeta_j|^2, \tag{30}$$

$$E_{\rm k}=\mathrm{Re}\left(\frac{1}{i\pi}\oint_{\gamma_u}\frac{c(z)}{z^3}dz\right)+2\sum_{j=1}^{J}\mathrm{Re}(\overline{\zeta_j}-\zeta_j). \tag{31}$$

Proof: Although the arguments are quite standard, they cannot be found in the literature for the Ablowitz-Ladik problem as far as I know, so I give some more detail for this part. Let ζ_j ($|\zeta_j|>1$) be the squares of the zeros of a, $j=1,\ldots,J$. We also denote $\overline{\zeta_j}=1/\zeta_j^*$. Then the function A,

$$A(z):=a(z)\prod_{j=1}^{J}\frac{z^2-\overline{\zeta_j}}{z^2-\zeta_j}, \tag{32}$$

is analytic in $|z|>1$ and has no zero. Furthermore it converges to 1 as $|z|\to 0$. By Cauchy's integral theorem we thus have

$$\frac{1}{2i\pi}\oint_{\gamma_u}\frac{\log A(z)}{z-\zeta}dz=0 \tag{33}$$

for any $|\zeta|<1$. On the other hand, the function $\overline{A}=\mathrm{Inv}(A)$,

$$\overline{A}(z)=\overline{a}(z)\prod_{j=1}^{J}\frac{z^{-2}-\overline{\zeta_j}^*}{z^{-2}-\zeta_j^*}, \tag{34}$$

is analytic in $|z|<1$ and has no zero. Thus, for any $|\zeta|<1$,

$$\frac{1}{2i\pi}\oint_{\gamma_u}\frac{\log\overline{A}(z)}{z-\zeta}dz=\log\overline{A}(\zeta). \tag{35}$$

Summing yields

$$\log\overline{A}(\zeta)=\frac{1}{2i\pi}\oint_{\gamma_u}\frac{\log(\overline{A}(z)A(z))}{z-\zeta}dz, \tag{36}$$

or, in terms of a and $\overline{a}$,

$$\log\overline{a}(\zeta)+\sum_{j=1}^{J}\log\frac{\zeta^{-2}-\overline{\zeta_j}^*}{\zeta^{-2}-\zeta_j^*}=\frac{1}{2i\pi}\oint_{\gamma_u}\frac{\log|a(z)|^2}{z-\zeta}dz-\sum_{j=1}^{J}\log|\zeta_j|^2. \tag{37}$$

We expand this expression with respect to $\zeta\to 0$ and collect the terms for each power of ζ. Applying lemma II.2 then establishes the equations

$$0=\frac{1}{2i\pi}\oint_{\gamma_u}\frac{\log|a(z)|^2}{z}dz-\sum_{j=1}^{J}\log|\zeta_j|^2, \tag{38}$$

$$C_1+\sum_{j=1}^{J}(\zeta_j^*-\zeta_j^{-1})=\frac{1}{2i\pi}\oint_{\gamma_u}\frac{\log|a(z)|^2}{z^3}dz, \tag{39}$$

where C_1 is given by Eq. (25). From the conservation relation (15), for any $z\in\mathbb{S}^1$ we have $|a|^2(z)=\exp(N_{tot}-c(z))$ so that Eqs. (38) and (39) also read like Eqs. (30) and (31).

E. Soliton

Equation (1) possesses soliton solutions, that is to say waves that propagate at constant velocities with constant envelopes. These solutions are of the form

$$q_{ns}(t)=\frac{\sinh(\mu)\exp[ik(n-x(t))+i\alpha(t)]}{\cosh[\mu(n-x(t))]}, \tag{40}$$

where

$$x(t)=x_0+2t\frac{\sinh(\mu)}{\mu}\sin(k), \tag{41}$$

$$\alpha(t)=\alpha_0+2t\left(\cosh(\mu)\cos(k)-1+\frac{k\sin(k)\sinh(\mu)}{\mu}\right). \tag{42}$$

The mass, velocity, and kinetic energy of the soliton are

$$N_s=2\mu,\quad U_s=2\frac{\sinh(\mu)}{\mu}\sin(k),\qquad E_{\mathrm{k},s}=-4\sinh(\mu)\cos(k), \tag{43}$$

respectively. The width of the envelope of the soliton is conversely proportional to its mass. The soliton solution [Eq. (40)] is associated with the following scattering data:

$$a_s(z)=\frac{z^2-\exp(ik+\mu)}{z^2-\exp(ik-\mu)},\quad b_s(z)=0. \tag{44}$$

a admits a unique pair of zeros in the outside of the unit circle that are denoted by $\exp(ik+\mu)$ and $-\exp(ik+\mu)$. The corresponding Jost functions are

$$\phi_{ns}(z)=\frac{z^n}{2\cosh\mu(n-1-x)}\times\begin{pmatrix}a_s(z)e^{\mu(n-1-x)}+e^{-\mu(n-1-x)}\\(1-a_s(z))ze^{-ik(n-x)-i\alpha}\end{pmatrix}, \tag{45}$$

$$\psi_{ns}(z)=\frac{z^{-n}}{2\cosh\mu(n-1-x)}\times\begin{pmatrix}(1-e^{-2\mu}a_s(z))z^{-1}e^{ik(n-x)+i\alpha}\\e^{\mu(n-1-x)}+a_s(z)e^{-\mu(n+1-x)}\end{pmatrix}. \tag{46}$$

III. INHOMOGENEOUS ABLOWITZ-LADIK CHAIN

A. Random on-site potential

We consider a perturbed Ablowitz-Ladik equation with a nonzero right-hand side:

$$iq_{nt}+q_{n+1}+q_{n-1}-2q_n+|q_n|^2(q_{n+1}+q_{n-1})=\varepsilon R_n(q). \tag{47}$$

The small parameter $\varepsilon\in(0,1)$ characterizes the amplitude of the perturbation. Here we assume that

$$R_n(q)=V_n q_n, \tag{48}$$

which means that Eq. (47) can be derived from the Hamiltonian

$$H=-2\sum_n \mathrm{Re}(q_n q_{n+1}^*)+\sum_n (2+\varepsilon V_n)\log(1+|q_n|^2). \tag{49}$$

Note that we could consider other kinds of perturbations, if they satisfy the condition "$R_n(q)q_n^*$ is real valued" (which implies that the system is conservative). We shall study another random problem in Sec. VI. In the framework of Eq. (48), the total mass N_{tot} and the total energy defined by

$$E_{\mathrm{tot}}:=E_{\mathrm{k}}+E_{\mathrm{c}}, \quad E_{\mathrm{c}}=\varepsilon\sum_n V_n \log(1+|q_n|^2) \tag{50}$$

are conserved. Note that $|E_{\mathrm{tot}}-E_{\mathrm{k}}|$ is uniformly bounded by $\varepsilon N_{tot}\|V\|_\infty$. The site-dependent potential V is assumed to be a bounded, zero-mean, stationary, and ergodic sequence of random variables. Its autocorrelation function is denoted by

$$\Gamma(n):=\mathbb{E}[V_0 V_n]=\mathbb{E}[V_{n'}V_{n'+n}], \tag{51}$$

where $\mathbb{E}$ stands for the statistical average with respect to the stationary distribution of V. We assume that the potential has enough decorrelation properties so that the series $\Sigma_{n=-\infty}^{\infty}|\Gamma(n)|^{1/2}$ is well defined and finite. We can then introduce the Fourier transform of the autocorrelation function of the potential V

$$d(\omega):=\sum_{n=-\infty}^{\infty}\Gamma(n)\exp(in\omega), \tag{52}$$

which is non-negative real valued since it is proportional to the power spectral density by the Wiener-Khintchine theorem [22]. For instance, if the random variables are independent and identically distributed (discrete white noise), then the spectrum of the potential is flat and given by $d(\omega)=\sigma^2=\mathbb{E}[V_n^2]$ for any ω.

We shall use the inverse scattering transform to study our problem. Indeed the random perturbation induces variations of the spectral data. Calculating these changes we are able to find the effective evolution of the field and calculate the characteristic parameters of the wave. We shall be interested in the effective dynamics of the soliton propagating over long times T/ε^2. The total mass and energy are conserved, but the discrete and continuous components evolve during the propagation. The evolution of the continuous component corresponding to the radiation will be found from the evolution equations of the Jost coefficients. The evolutions of the soliton parameters will then be derived from the conservation of the total mass and energy.

B. Evolution of the scattering data

We now describe the evolutions of the Jost coefficients a and b during the propagation. They satisfy the exact equations [23]

$$\frac{\partial a}{\partial t}=-i\varepsilon\sum_n \frac{W(\psi_{n+1}(z),F(q_n)\phi_n(z))}{W(\overline{\psi}_{n+1}(z),\psi_{n+1}(z))}, \tag{53}$$

$$\frac{\partial b}{\partial t}=i\omega(z)b+i\varepsilon\sum_n \frac{W(\overline{\psi}_{n+1}(z),F(q_n)\phi_n(z))}{W(\overline{\psi}_{n+1}(z),\psi_{n+1}(z))}, \tag{54}$$

where $F(q_n)=\begin{pmatrix}0 & R_n(q)\\ R_n^*(q) & 0\end{pmatrix}$. These equations will be needed below when calculating the radiative mass and energy generated by the moving soliton. After some algebra this system simplifies into

$$\frac{\partial a}{\partial t}=-i\varepsilon(a\gamma_1+b\gamma_2), \tag{55}$$

$$\frac{\partial b}{\partial t}=i\omega(z)b+i\varepsilon(-a\gamma_2^*+b\gamma_1), \tag{56}$$

where

$$\gamma_1(t)=\sum_n \frac{\psi_{1,n+1}\psi_{2,n}^*R_n^*(q)+\psi_{2,n+1}\psi_{1,n}^*R_n(q)}{W_{n+1}}, \tag{57}$$

$$\gamma_2(t)=\sum_n \frac{R_n^*(q)\psi_{1,n}\psi_{1,n+1}-R_n(q)\psi_{2,n}\psi_{2,n+1}}{W_{n+1}}, \tag{58}$$

$$W_{n+1}(t)=|\psi_{1,n+1}|^2+|\psi_{2,n+1}|^2=\prod_{m=n+1}^{\infty}(1+|q_m|^2)^{-1}. \tag{59}$$

The time independence of $|a|^2+|b|^2$ for any $z\in\mathbb{S}^1$ is conserved by these equations, which holds true as soon as the total mass is preserved.

C. Adiabatic approximation

The adiabatic approximation consists of assuming *a priori* that, while the soliton exists, its evolution and the one of the radiated wave do not interact. More precisely, we assume that the time evolutions of the Jost coefficients a and b given by Eq. (53) depend only on the components of the functions γ_1 and γ_2 which are associated with the soliton. We can then carry out calculations under this approximation, since it reduces the analysis which provide an expression of the solution q_n. *A posteriori*, we check for consistency that this approximation is actually justified in the asymptotic framework $\varepsilon\to 0$. More exactly we show that the components of the functions γ_1 and γ_2 which correspond to the interplay between the computed radiation and the soliton, or else which originate from the sole effect of the radiation, can be considered as negligible terms for the soliton evolution.

D. Asymptotic regime

Let $T>0$. Let us denote by Ω_T^ε the set of realizations of the potential $(V_n)_n$ such that the wave after propagation over $[0,T/\varepsilon^2]$ consists of one soliton plus some radiation. We denote by μ^ε and k^ε the rescaled processes defined on Ω_T^ε by

$\mu^\varepsilon(t)=\mu(t/\varepsilon^2)$ and $k^\varepsilon(t)=k(t/\varepsilon^2)$ (i.e. the parameters of the transmitted soliton at time t/ε^2), and on the complementary set $\Omega_T^{\varepsilon c}$ by $\mu^\varepsilon(t)=0$ and $k^\varepsilon(t)=0$. We can now state our main convergence result, whose proof is given in Appendix A.

Proposition III.1. Under the adiabatic approximation, the following assertions hold true for any $T>0$:

(1) $\liminf_{\varepsilon\to 0}\mathbb{P}(\Omega_T^\varepsilon)=1$.

(2) The $\mathbb{R}^2$-valued process $(\mu^\varepsilon(t),k^\varepsilon(t))_{t\in[0,T]}$ converges in probability to the $\mathbb{R}^2$-valued deterministic function $(\mu_l(t),k_l(t))_{t\in[0,T]}$ which satisfies the system of ordinary differential equations

$$\frac{d\mu_l}{dt}=F(\mu_l,k_l),\quad \mu_l(0)=\mu_0,\qquad \frac{dk_l}{dt}=G(\mu_l,k_l),\quad k_l(0)=k_0. \tag{60}$$

The functions F and G are equal to

$$F(\mu,k)=-\frac{1}{2}\int_0^{2\pi}C(\mu,k,\theta)d\theta, \tag{61}$$

$$G(\mu,k)=-\frac{1}{2\sinh(\mu)\sin(k)}\int_0^{2\pi}(\cosh(\mu)\cos(k)-\cos(2\theta))C(\mu,k,\theta)d\theta, \tag{62}$$

where the function C is the mass density scattered by the soliton with parameters (μ,k) per unit time. The parameter θ is related to the spectral parameter z through $z=e^{i\theta}$. The exact expression of C is the following:

$$C(\mu,k,\theta)=\frac{\pi\sinh\mu}{16\mu\cosh\left(\frac{\omega_1\pi}{2\mu}\right)^2\sin(k)}\times\frac{\sin(\omega_2/2)^4 d(\omega_2)}{(\cosh(\mu)-\cos(2\theta-k))^2}, \tag{63}$$

where the functions ω_1 and ω_2 are defined by

$$\omega_1(\mu,k,\theta)=\mu\frac{\cosh(\mu)\cos(k)-\cos(2\theta)}{\sinh(\mu)\sin(k)},$$

$$\omega_2(\mu,k,\theta)=\omega_1(\mu,k,\theta)+k-2\theta. \tag{64}$$

The first assertion of the proposition means that the event ‘‘the transmitted wave consists of one soliton plus some radiation’’ occurs with very high probability for small ε, while the second assertion gives the effective evolution equation of the parameters of the transmitted soliton in the asymptotic framework $\varepsilon\to 0$.

IV. EFFECTIVE EVOLUTION OF THE SOLITON PARAMETERS

This section is devoted to the study of the evolutions of the parameters of the transmitted soliton. By proposition III.1 these evolutions are given by Eq. (60). We aim at exhibiting the relevant characteristics of this deterministic system of ordinary differential equations.

A. Linear regime in the approximation $\mu_0\ll 1$

System (60) can then be simplified to a good approximation:

$$\frac{d\mu}{dt}=-\frac{d(2k)}{2\sin(k)}\mu,\qquad \frac{dk}{dt}=-\frac{d(2k)}{6}\frac{\mu^3}{\tan(k)}, \tag{65}$$

with the initial conditions imposed by the incoming soliton: $\mu(0)=\mu_0$ and $k(0)=k_0$. It thus appears that the velocity U of the soliton [equal to $2\sin(k)\sinh(\mu)/\mu\simeq 2\sin(k)$] is almost constant during the propagation, while the mass N (equal to 2μ) decreases exponentially:

$$\mu(t)\simeq\mu_0\exp\left(-\frac{t}{T_1}\right),\quad T_1=\frac{2\sin(k_0)}{d(2k_0)}. \tag{66}$$

Accordingly the localization length that is defined for a soliton with velocity U as $L_1=UT_1$ is equal to

$$L_1=\frac{4\sin(k_0)^2}{d(2k_0)}. \tag{67}$$

The spectrum of the radiation is concentrated around the spectral parameter $\theta=-k_0/2$ (and $-k_0/2+\pi$). This means that the radiation oscillates as $\exp(-ik_0n)$. More precisely, the mass density of scattered wave is

$$C\left(\theta=-\frac{k_0}{2}+\mu x\right)=\frac{\pi d(2k_0)}{2\cosh(\pi x)^2\sin(k_0)}. \tag{68}$$

It can be noted that, in the limit case $\mu_0\to 0$, the incoming soliton can be approximated by a linear wave packet:

$$q_n(t)\simeq\int_{-\infty}^{+\infty}d\kappa\,\hat\phi_0(\kappa)e^{i\kappa n-i4\sin^2(\kappa/2)t}$$

with

$$\hat\phi_0(\kappa)=\frac{1}{4}\cosh^{-1}\left(\frac{\pi}{4}\left(\frac{\kappa-k_0}{\mu_0}\right)\right). \tag{69}$$

Note that the dispersion relation for the linear discrete Schrödinger equation reads $\omega(\kappa)=4\sin^2(\kappa/2)$. The spectrum $\hat\phi_0$

of the soliton is sharply peaked about k_0, so that the localization length also reads as $L_1=\omega(2k_0)/d(2k_0)$.

If $k_0 \ll 1$, then we regain the well-known continuum limit. The continuum dispersion relation reads $\omega(\kappa)=\kappa^2$. The spectrum of the soliton has a carrier wave number k_0. Furthermore the spectrum of the scattered wave packet is peaked about the spectral parameter $-k_0/2$, which corresponds to the wave number $-k_0$. These statements are in agreement with the linear approximation. The localization length $L_1=\omega(2k_0)/d(2k_0)$ corresponds to the localization length of a monochromatic wave with wave number k_0 scattered by a slab of linear random medium. We have thus recovered the results stated in (Ref. [24] theorem 4.1), where the authors showed that, in such a situation, for ε small enough, the transmission coefficient T^ε satisfies, with probability 1:

$$\lim_{L\to\infty} \frac{1}{L} \log|T^\varepsilon|^2(L) = -\frac{\varepsilon^2}{L_1} + O(\varepsilon^3). \tag{70}$$

B. Nonlinear regime in the approximation $\mu_0 \gg 1$

System (60) can then be simplified:

$$\frac{d\mu}{dt} = -\frac{3d\left(\frac{\mu}{\tan(k)}\right)\pi^2 e^{-\mu}}{64\mu \cosh\left(\frac{\pi}{2\tan(k)}\right)^2 \sin(k)},$$

$$\frac{dk}{dt} = -\frac{3d\left(\frac{\mu}{\tan(k)}\right)\pi^2 e^{-\mu}}{64\mu \cosh\left(\frac{\pi}{2\tan(k)}\right)^2 \sin(k)\tan(k)}, \tag{71}$$

with the initial conditions $\mu(0)=\mu_0$ and $k(0)=k_0$. The mass density of the scattered wave is

$$C(\theta) = \frac{d\left(\frac{\mu}{\tan(k)}\right)\pi e^{-\mu}}{8\mu \cosh\left(\frac{\pi}{2\tan(k)}\right)^2 \sin(k)} \sin^4\left(\frac{\mu}{\tan(k)} + k - 2\theta\right). \tag{72}$$

The soliton emits radiation whose spectrum covers all frequencies with a $\sin^4$ form centered at $\mu/\tan(k)+k$ modulo 2π. It can be readily checked that $\exp(\mu)\cos(k)$ is constant during the propagation, which means that the mass of the soliton converges to the limit value N_{lim},

$$N_{lim} = 2\mu_{lim} = 2\mu_0 + 2\log(\cos(k_0)), \tag{73}$$

while the velocity of the soliton decreases to 0. When k becomes small, system (71) reads, in simplified form,

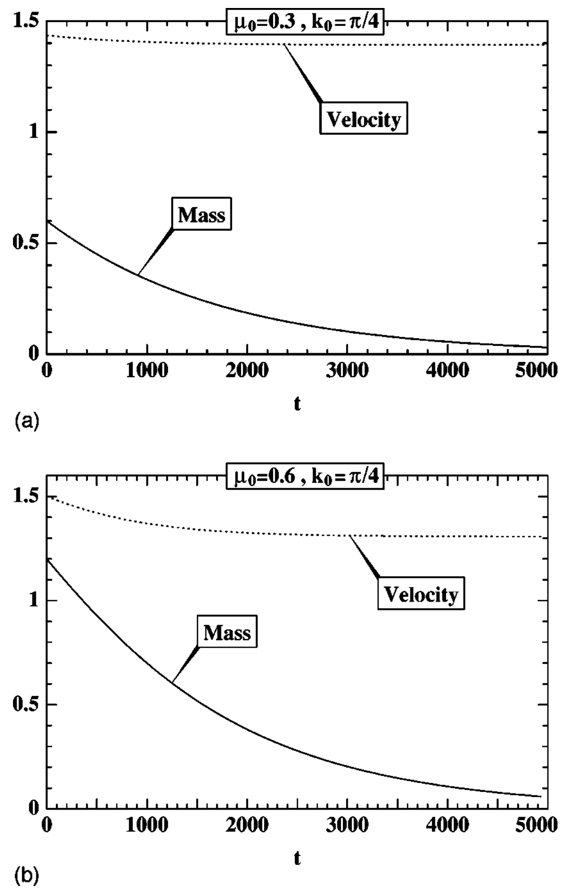

FIG. 1. Mass and velocity of the soliton during the propagation. The lines correspond to the theoretical values computed from system (60). We assume that $\sigma^2=\frac{1}{12}10^{-2}$. The initial values of the soliton parameters are $\mu_0=0.3$ and $k_0=\pi/4$ (a) and $\mu_0=0.6$ and $k_0=\pi/4$ (b). The velocity is almost constant, while the mass decays exponentially.

$$\frac{d\mu}{dt} = -\frac{3d\left(\frac{\mu}{k}\right)\pi^2 \exp\left(-\mu-\frac{\pi}{k}\right)}{16\mu k},$$

$$\frac{dk}{dt} = -\frac{3d\left(\frac{\mu}{k}\right)\pi^2 \exp\left(-\mu-\frac{\pi}{k}\right)}{16\mu k^2}. \tag{74}$$

Since μ converges to $\mu_{lim}=\mu_0+\log(\cos(k_0))$, this means that the decay of k is governed by

$$\frac{dk}{dt} = -\frac{3\pi^2\exp(-\mu_{lim})}{16\mu_{lim}} \frac{d\left(\frac{\mu_{lim}}{k}\right)\exp\left(-\frac{\pi}{k}\right)}{k^2}. \tag{75}$$

The limit behavior for large t of the parameter k depends on the high frequency behavior of the Fourier transform of the autocorrelation function of the potential V. The exact decay rate of the velocity results from the competition between the terms $d(\mu_{lim}/k)$ and $\exp(-\pi/k)$ in Eq. (75). If the spectrum

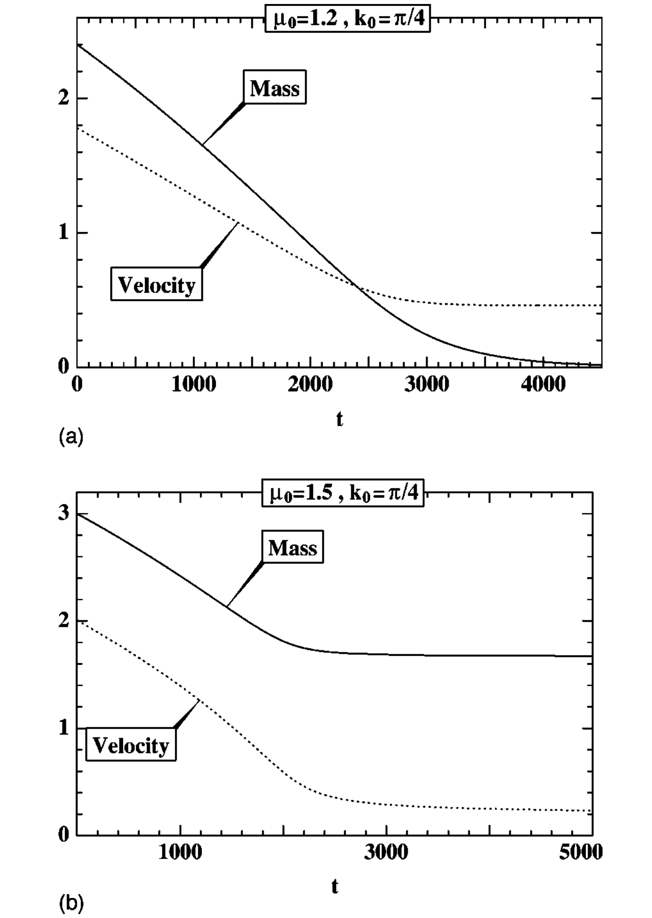

FIG. 2. Mass and velocity of the soliton during the propagation. The lines correspond to the theoretical values computed from system (60). We assume that $\sigma^2=\frac{1}{12}10^{-2}$. The initial values of the soliton parameters are $\mu_0=1.2$ and $k_0=\pi/4$ (a) and $\mu_0=1.5$ and $k_0=\pi/4$ (b). In both pictures, the mass and velocity begin by decaying almost linearly. After this transition regime, the pictures become very different, although the initial values of the parameters are very close. In picture (a), the velocity tends to a constant positive value, and the mass decays exponentially to zero. In picture (b), the mass tends to a constant positive value, and the velocity decays to zero at logarithmic rate.

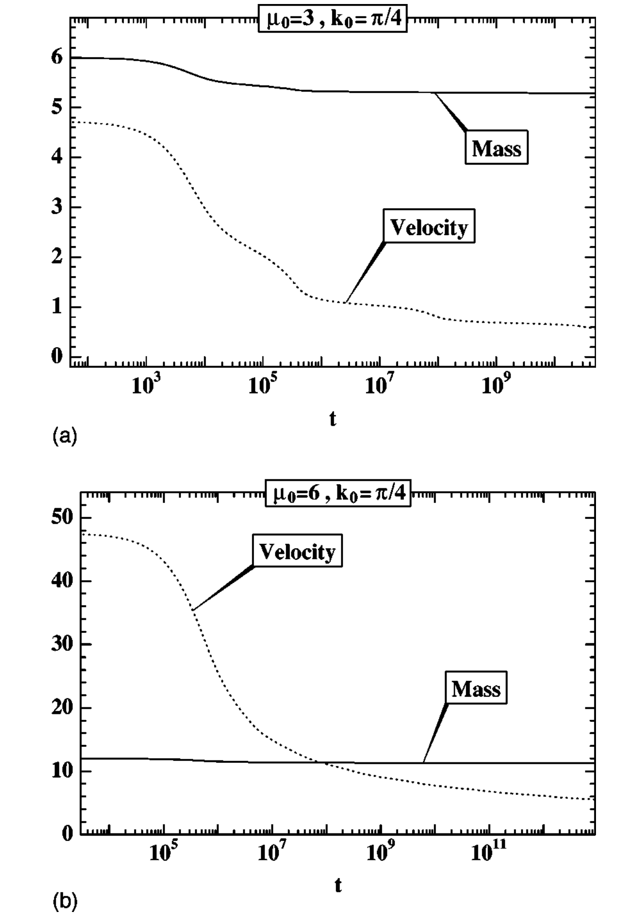

FIG. 3. Mass and velocity of the soliton during the propagation. The lines correspond to the theoretical values computed from system (60). We assume that $\sigma^2=\frac{1}{12}10^{-2}$. The initial values of the soliton parameters are $\mu_0=3$ and $k_0=\pi/4$ (a) and $\mu_0=6$ and $k_0=\pi/4$ (b). The mass goes to the value $N_0+2\log[\cos(k_0)]=N_0-0.69$, and the velocity decays at a logarithmic rate.

of the potential $d(\omega)$ decays slower than $\exp(-\pi\omega/\mu_{lim})$, then the exponential term is the smallest one, and consequently imposes the decay rate of k:

$$k(t)\simeq\frac{\pi}{\log t}. \tag{76}$$

This logarithmic rate actually represents the maximal decay of the velocity. Whatever the potential V, the terms of the right-hand sides of Eq. (75) have at least an exponential decay of the type $\exp(-\pi/k)$, which implies $\liminf_{t\to\infty} k(t)\times\log(t)\geqslant\pi$. However, the decay rate may be much slower. For instance, assume that the spectrum of V has Gaussian shape so that $d(\omega)=\sigma^2\exp(-l_c^2\omega^2)$. Then the velocity decreases as the square root of the logarithm of t:

$$k(t)\simeq\frac{\mu_{lim}l_c}{\sqrt{\log t}}. \tag{77}$$

The decay rate $(\log t)^{-1/2}$ is imposed by the shape of the tail of the spectrum of the random potential V. If the spectrum decays faster than a Gaussian, then the regime corresponding to Eq. (77) will be still slower. Conversely, if the spectrum decays slower than any exponential, then one can only observe regime (76).

C. Numerical resolution of the effective system

In the above paragraphs we have reported two domains which are stable with respect to the evolutions of the parameters of the transmitted soliton. We aim at showing here that these regimes are not only stable, but attractive. In order to prove this statement, we are going to solve numerically system (60) for different incoming solitons, without any assumption about the values of the initial parameters μ_0 and k_0. For simplicity, in this section we assume that the spectrum of the random potential is flat $d(\omega)\equiv\sigma^2$, which means that the potential $(V_n)_{n\in\mathbb{Z}}$ is a sequence of independent and identically distributed random variables and $\sigma^2 = \mathbb{E}[V_n^2]$.

Figures 1–3 plot the evolutions of the parameters of the transmitted soliton as functions of the duration t. The parameter k_0 is chosen at some fixed value for all figures, equal to $\pi/4$, but the initial mass $N_0 = 2\mu_0$ varies from 0.6 to 12. The striking point is that two different behaviors can be put into evidence, and that they are separated from each other by a critical value $2\mu_c$ of the initial mass $2\mu_0$.

When $\mu_0 < \mu_c$ [Figs. 1 and 2(a)], after a transition regime where the mass and the velocity decrease as powers, the velocity reaches a stable value U_{lim}. This limit value is very close to the initial value U_0 when $\mu_0 \ll \mu_c$. Once the velocity is stable, the mass decreases exponentially with the localization length U_{lim}/σ^2; this regime was described in Sec. IV A.

When $\mu_0 > \mu_c$ [Figs. 2(b) and 3], after a transition regime where both the mass and the velocity decrease, the mass reaches a stable value N_{lim} which is equal to $N_0 - 2\log(\cos(k_0))$ if $\mu_0 \gg \mu_c$. Once the mass is stable, the velocity decreases as $\pi/\log t$, as described in Sec. IV B.

One can also note that the critical point μ_c is unstable. We practically always observe one of the limit behaviors described in Secs. IV A and IV B.

We would also like to comment upon the oscillations of the velocity that can be observed in the left picture of Fig. 3. These oscillations are due to the discreteness, and they appear in the regime when $\mu > \mu_c$, but μ is not very large, so that system (71) is not strictly fulfilled. One must then reconsider the original system (60), and consider the asymptotic $k \to 0$ and consider that μ is of order 1. After some algebra one establishes that system (60) can then be simplified into

$$\frac{d\mu}{dt} = -\frac{\pi \sinh^{1/2}(\mu)}{64 w(\mu) k^{1/2}} d\left(\frac{w(\mu)}{k}\right) \exp\left(-\frac{\pi w(\mu)}{k\mu}\right) h(\mu,k), \tag{78}$$

$$\frac{dk}{dt} = -\frac{\pi \sinh^{1/2}(\mu)}{64 \mu k^{3/2}} d\left(\frac{w(\mu)}{k}\right) \exp\left(-\frac{\pi w(\mu)}{k\mu}\right) h(\mu,k),$$

where

$$h(\mu,k) = \frac{\cos\left(2\frac{w(\mu)}{k} + \frac{1}{2}\arctan\left(\frac{2\mu}{\pi}\right)\right)}{(1+4\mu^2\pi^{-2})^{1/4}} + 4\frac{\cos\left(\frac{w(\mu)}{k} + \frac{1}{2}\arctan\left(\frac{\mu}{\pi}\right)\right)}{(1+\mu^2\pi^{-2})^{1/4}} + 3,$$

$$w(\mu) = \mu(\cosh(\mu) - 1)/\sinh(\mu).$$

The first two terms of $h(\mu,k)$ are responsible for the oscillations. Indeed they are of the form $\cos(w/k)$ with (almost) constant w, so they oscillate as $k \to 0$.

V. NUMERICAL SIMULATIONS

The results in the previous sections are theoretically valid in the limit case $\varepsilon \to 0$, where the amplitudes of the perturbations go to zero and the size of the random system goes to infinity. In this section we aim to show that the asymptotic behaviors of the soliton can be observed in numerical simulations in the case where ε is small, more precisely smaller than any other characteristic scale of the problem. We use a fourth-order Runge-Kunta method to simulate the perturbed nonlinear Schrödinger equation (47). This numerical algorithm provides accurate and stable solutions to a large class of systems of ordinary and partial differential equations (Ref. [25], p. 346). We checked the accuracy of the method by evaluating the quantities E_k and N in the absence of a random potential $(\varepsilon = 0)$. They were conserved to a relative error less than 10^{-4}.

Let Δt be the elementary time step. We denote the initial wave solution by $(q_n^0)_{n=0,\dots,M-1}$. By induction we compute $q^{j+1} := [q_n((j+1)\Delta t)]_{n=0,\dots,M-1}$ from $q^j := (q_n(j\Delta t))_{n=0,\dots,M-1}$. Since the time domain is planned to be very long, of order ε^{-2}, the solution will propagate over distances of order ε^{-2}, so that we would have to take a computational domain of size $M \sim \varepsilon^{-2}$. In order to deal with a tractable problem, we use a shifting computational domain which is always centered at the center of mass of the solution. Moreover, we impose boundaries of this domain which absorb outgoing waves. This can be readily achieved by adding a complex potential which is smooth so as to reduce reflections. We choose to substitute the complex potential $\tilde{V} = V - iV_{abs}$ for the random potential V,

$$V_{abs,n} = \begin{cases} V_{absmax} \sin^2\left(\frac{\pi}{2}\frac{M_0 - n}{M_0}\right) & \text{if } 0 \le n < M_0 \\ 0 \quad \text{if } M_0 \le n \le M - 1 - M_0 \\ V_{absmax} \sin^2\left(\frac{\pi}{2}\frac{M_0 + n + 1 - M}{M_0}\right) & \text{if } M - 1 - M_0 < n \le M - 1, \end{cases} \tag{79}$$

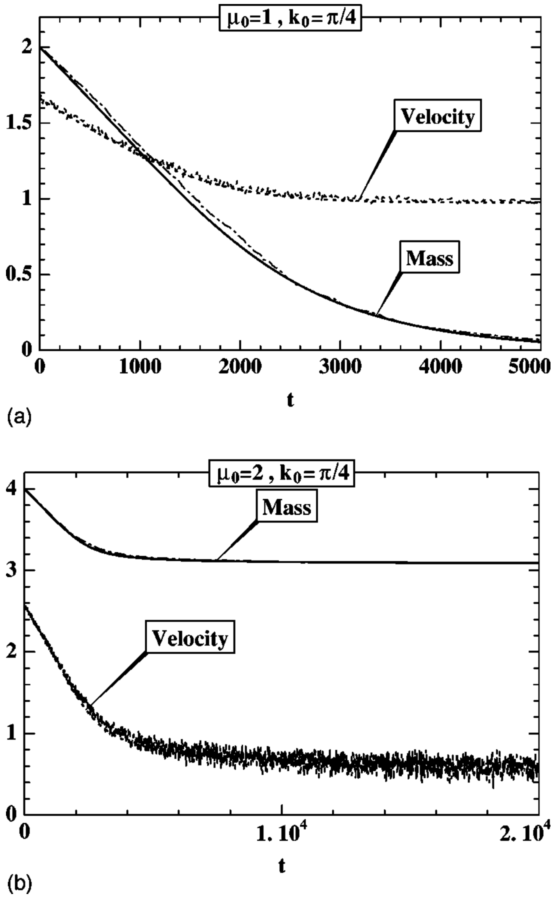

FIG. 4. Mass and velocity of the soliton during the propagation. The thick lines correspond to the theoretical values computed from system (60). The thin lines correspond to a numerical simulation of the Ablowitz-Ladik equation, with a random potential with an amplitude equal to $\varepsilon=0.1$. In picture (a) the initial values of the soliton parameters are $\mu_0=1$ and $k_0=\pi/4$, which correspond to the linear regime where the mass decays exponentially to zero and the velocity tends to a constant positive value. In picture (b) the initial values of the soliton parameters are $\mu_0=2$ and $k_0=\pi/4$, which correspond to the nonlinear regime where the mass tends to a constant positive value while the velocity logarithmically decays to zero.

where $M-1$ (0) is the left (right) end of the computational domain, and $[0,M_0]$ ($[M-1-M_0,M-1]$) is the left (right) absorbing slab.

We assume in this section that the random potential V_n is a sequence of independent and identically distributed variables, which obey uniform distributions over the interval $[-1/2,1/2]$, so that $d(\omega)\equiv\sigma^2=1/12$, We take $\varepsilon=0.1$. In such conditions $\sigma^2\varepsilon^2=\frac{1}{12}10^{-2}$. The time T will be chosen so large (of order ε^{-2}) that we can observe the effect of the small perturbation εV_n. We measure the mass and the kinetic energy, of the solution during the propagation, as well as the envelope of the transmitted solution, that we can compare with the envelope of the incident soliton. The mass $N(j\Delta t)$ and the energy $E_{\mathrm{k}}(j\Delta t)$ are computed at time $j\Delta t$ from the data $(q_n(j\Delta t))_{n=0,\ldots,M-1}$ as

$$N(j\Delta t)=2\sum_{n=0}^{M-1}\log(1+|q_n(j\Delta t)|^2),$$

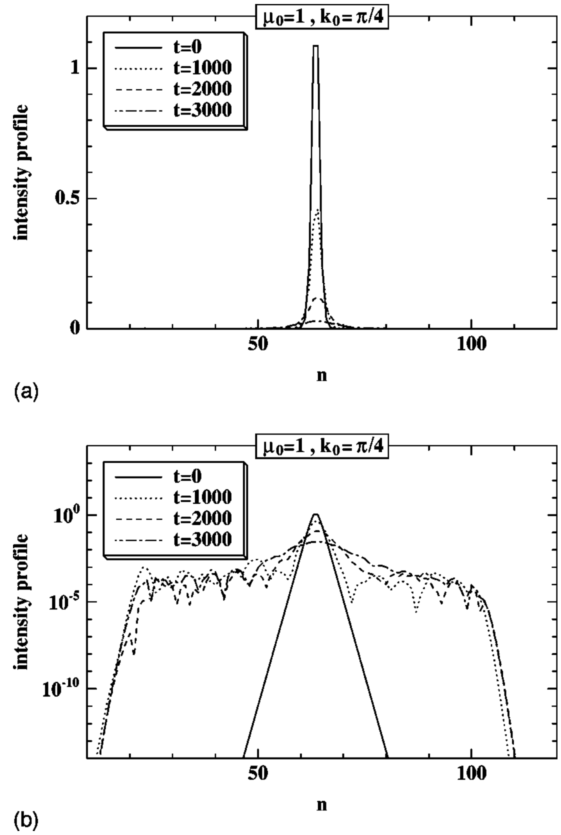

FIG. 5. Intensity profiles of the solutions at different times. The coordinate n is shifted around the center of mass. The initial wave is a soliton with parameters $\mu_0=1$ and $k_0=\pi/4$. The same data are plotted on a linear scale in picture (a), and on a logarithmic scale in picture (b). The cutoff that can be observed in picture (b) at the boundaries of the domain originates from the absorbing potential V_{abs}.

$$E_{\mathrm{k}}(j\Delta t)=-2\,\mathrm{Re}\left(\sum_{n=0}^{M-2}q_n(j\Delta t)q_{n+1}^*(j\Delta t)\right). \tag{80}$$

We finally deal with the set of data $(E_{\mathrm{k}}(j\Delta t))_j$ in order to compute the velocity of the soliton, which can be computed by Eq. (43):

$$U(j\Delta t)=\frac{\sqrt{16\sinh^2(N(j\Delta t)/2)-E_{\mathrm{k}}^2(j\Delta t)}}{N(j\Delta t)}. \tag{81}$$

We perform different simulations where the initial wave at time $t=0$ is a pure soliton with parameters (μ_0,k_0) centered at $x_s=M/2$. In the first one we simulate the homogeneous nonlinear Schrödinger equation (1), which admits as an exact solution (40). We can therefore check the accuracy of the numerical method, since we can see that the computed solution maintains a very close resemblance to the initial soliton (data not shown), while the mass and velocity are almost constant. The other simulations are carried out with various values of the initial parameters (μ_0,k_0) and different realizations of the random potential with $\varepsilon=0.1$. The simulated evolutions of the soliton parameters are presented in Fig. 4, and compared with the theoretical evolutions given by Eq. (60) on the scale t/ε^2.

It thus appears that the numerical simulations are in very good agreement with the theoretical results. The simulated masses follow very closely the theoretical ones. This is partly due to the fact that the perturbed equation preserves the total mass,

$$N_{tot}=2\mu+\frac{1}{2\pi}\int_0^{2\pi}c(e^{i\theta})d\theta, \tag{82}$$

where $c(\cdot)$ is the density of the scattered mass. This implies stability for the parameter μ and the mass of the soliton. It also appears that the velocity follows theoretical curves, but also presents quickly varying fluctuations around the theoretical values. This is in fact not surprising. Indeed the perturbed equation preserves the total energy, which can be expressed from Eqs. (31) and (50) as

$$E_{tot}=-4\sinh(\mu)\cos(k)+\frac{1}{\pi}\int_0^{2\pi}c(e^{i\theta})\cos(2\theta)d\theta+\varepsilon\sum_n V_n\log(1+|q_n|^2). \tag{83}$$

The last term is negligible in the asymptotic framework $\varepsilon\to 0$, but when $\varepsilon=0.1$ it gives rise to local fluctuations of the parameter k and of the instantaneous velocity of the soliton.

Figure 5 plots the envelopes of the solution at different times corresponding to one of the simulations, which shows that the wave keeps the basic form of a soliton although it loses some mass. All these results confirm that system (60) describes with accuracy the transmission of a soliton in a nonlinear Ablowitz-Ladik chain with small random perturbations.

VI. A SECOND RANDOM PROBLEM

We would like to briefly present a second model that describes a random Ablowitz-Ladik chain that could be of interest for applications to discrete spatial solitons in waveguide arrays, for example. We have considered a random on-site potential in the above sections, that corresponds to Hamiltonian system (49). However, it often happens that the randomness originates from the coupling coefficients, so that the underlying Hamiltonian is

$$H=-2\sum_n (1+\varepsilon\Lambda_n)\mathrm{Re}(q_nq^*_{n+1})+2\sum_n \log(1+|q_n|^2), \tag{84}$$

where Λ_n are real-valued random variables. In the planar waveguide framework [10], the tunnel coupling coefficient $1+\varepsilon\Lambda_n$ is proportional to the gap between the guides n and $n+1$. Note that we have normalized the average coupling coefficient to 1, and that $\varepsilon\Lambda_n$ stands for the zero-mean fluctuations. If we denote the transverse coordinate of the nth guide by λ_n, we have $1+\varepsilon\Lambda_n=\lambda_{n+1}-\lambda_n$. The system that governs the evolution of q_n is

$$iq_{nt}+(q_{n+1}(1+\varepsilon\Lambda_n)+q_{n-1}(1+\varepsilon\Lambda_{n-1}))(1+|q_n|^2)-2q_n=0. \tag{85}$$

In such conditions the total mass and the energy defined as Eq. (84) are preserved. We can then perform the very same study as in the case of a random on-site potential, and come to the same conclusion as the one stated in proposition III.1. The only difference comes from the fact that the expression of the scattered mass density is not Eq. (63), but a more intricate expression. Nevertheless we can study this expression in some relevant configurations.

We have found that the mass density scattered by a soliton with initial parameters k_0 and $\mu_0\ll 1$ has the same shape as one corresponding to the random potential configuration (up to a factor 4). The spectrum of the radiation is concentrated around the spectral parameter $\theta=-k_0/2$:

$$C\left(\theta=-\frac{k_0}{2}+\mu x\right)=\frac{2\pi d(2k_0)}{\cosh(\pi x)^2\sin(k_0)}. \tag{86}$$

Accordingly the localization length for a low-amplitude soliton with velocity $U=2\sin(k_0)$ is equal to

$$L_2=\frac{\sin(k_0)^2}{d(2k_0)}. \tag{87}$$

If the random coupling coefficients Λ_n are of the form $1+\varepsilon\Lambda_n=\lambda_{n+1}-\lambda_n$, with independent random variables λ_n with variance $\varepsilon^2\sigma^2$, then $d(2k_0)=4\sin(k_0)^2\sigma^2$. This implies that the localization length is independent of the soliton parameters: $L_2=\sigma^{-2}/4$.

On the other hand, we have found that in the strong nonlinear regime $\mu_0\gg 1$ the mass of the soliton converges to the value $N_0+2\log(\cos(k_0))$ while the velocity slowly decays to zero. This regime is very similar to the one discussed in Sec. IV B for the random on-site potential.

VII. CONCLUSIONS

We have applied two types of random perturbations to the integrable lattice nonlinear Schrödinger equation. We have studied the propagation of a soliton with mass $N_0=2\mu_0$ and velocity $U_0=2\sinh(\mu_0)\mu_0^{-1}\sin(k_0)$ in these random nonlinear chains. We have found that there exists a critical value of the initial mass of the soliton below which we observe an exponential decay of the mass, and above which an original nonlinear regime prevails which involves the convergence of the mass of the soliton to a calculable positive value and the slow decay of the velocity.

More exactly, in case of a small initial mass N_0, we have proved that the velocity of the soliton is almost constant, while the mass of the soliton decays exponentially with the size of the system. We have computed the localization length for both types of perturbations. In the case of a large initial mass N_0, we have shown that the mass of the soliton converges to the value $N_0+2\log(\cos(k_0))$. Furthermore the velocity is found to decrease at logarithmic or sublogarithmic rates to 0.

ACKNOWLEDGMENT

The author is grateful to F. Kh. Abdullaev for useful and stimulating discussions.

APPENDIX: DERIVATION OF THE EFFECTIVE SYSTEM

In this section we outline the main steps of the proof of proposition III.1, which closely follows the strategy developed in Ref. [8], and we shall underline the key points.

(1) *Prove the stability of the zero of the Jost coefficient* a. The zero corresponds to the soliton. This part strongly relies on the analytical properties of a in the outside of the unit circle, and it is very similar to the corresponding part in Ref. [8]. Basically we apply Rouché's theorem so as to prove that the number of zeros is constant. This method is efficient to prove that the zero is preserved, but it does not bring control on its precise location in the outside circle. This step is not sufficient to compute the variations of the soliton parameters.

(2) *Compute the amount of radiation, and then the variations of the soliton parameters*. Under the adiabatic approximation, we solve the evolution equations (53) so that we obtain a closed-form expression of the ratio b/a. More exactly, the scattering data $\tilde{b}/a(t,z)=b/a(t,z)e^{-i\omega(z)t}$ at time t_0/ε^2 is given by

$$\frac{\tilde{b}}{a}\left(\frac{t_0}{\varepsilon^2},z\right)=-i\varepsilon\int_{-\infty}^{t_0/\varepsilon^2}\gamma_3 e^{-i\omega(z)t}dt, \tag{A1}$$

$$\gamma_3(t,z)=\sum_n V_n z^{2n+1}e^{-ik(n-x_s(t))-i\alpha_s(t)}\sinh(\mu)\,\gamma_4^*(n-x_s(t),z) \tag{A2}$$

$$\gamma_4(y,z)=\frac{(1-e^{-2\mu}a_s(z))^2z^{-2}e^{ik+\mu}-e^{2\mu y}-a_s^2(z)e^{-2\mu(y+1)}-a_s(z)(1+e^{-2\mu})}{4\cosh[\mu(y-1)]\cosh(\mu y)\cosh[\mu(y+1)]}, \tag{A3}$$

$$a_s(z)=\frac{z^2-e^{ik+\mu}}{z^2-e^{ik-\mu}}, \tag{A4}$$

where $x_s(t)$ and $\alpha_s(t)$ are the position of the center of the soliton and the phase of the soliton at time t defined by Eq. (A8). From Eq. (A1) we can estimate the amount of radiation which is emitted during some time interval in terms of mass and energy thanks to Eqs. (30) and (31). We are then able to deduce the evolution equations of the soliton parameters by using the conservations of the total mass and energy. For times of order $O(1)$, since N_{tot} and E_{tot} are conserved, the variations $\Delta(\cdots)$ of the relevant quantities are linked together by the relations

$$0=2\Delta\mu+\frac{1}{2\pi}\int\Delta c(e^{i\theta})d\theta, \tag{A5}$$

$$0=-4\Delta(\sinh(\mu)\cos(k))+\frac{1}{\pi}\int_0^{2\pi}\Delta c(e^{i\theta})\cos(2\theta)d\theta+\varepsilon\Delta(E_c). \tag{A6}$$

$\Delta c(e^{i\theta})$ is of order ε^2, but the last term in the expression of the total energy is of order ε. Thus our strategy is not efficient for estimating the variations of the soliton parameters for times of order $O(1)$. Let us now consider times of order $O(\varepsilon^{-2})$. $\Delta c(e^{i\theta})$ is now of order 1, while the last term in the expression of the total energy is bounded above by $2\varepsilon N\|V\|_\infty$, which is uniformly negligible as $\varepsilon\to 0$. Thus we can efficiently compute the long-time behaviors of the soliton parameters in the asymptotic framework $\varepsilon\to 0$, when the last term in the expression of the total energy is uniformly negligible. Using probabilistic limit theorems, we then find that the soliton parameters converge in probability to nonrandom functions which satisfy system (60).

(3) *Compute the form of the scattered wave*. Given the scattering data, we can reconstruct the wave by the inverse scattering technique presented in Sec. II C. Under the adiabatic approximation, neglecting terms of higher order, the total wave is given by the sum $q(t/\varepsilon^2)=q_S(t/\varepsilon^2)+q_L(t/\varepsilon^2)$, where q_S is a soliton of mass $2\mu(t/\varepsilon^2)$ and velocity $2\sinh(\mu)\sin(k(t/\varepsilon^2))/\mu$:

$$q_{S,n}\left(\frac{t}{\varepsilon^2}\right)=\frac{\sinh(\mu)\exp[ik(n-x_s)+i\alpha_s]}{\cosh[\mu(n-x_s)]}. \tag{A7}$$

x_s and α_s are, respectively, the position and the phase of the soliton at time t/ε^2

$$x_s=\frac{1}{\mu}\log\left(\frac{1}{\sinh(\mu)}|\overline{c_r}(t/\varepsilon^2)|\right),\quad \alpha_s=\arg(\overline{c_r}(t/\varepsilon^2))+kx_s, \tag{A8}$$

and q_L admits the expression

$$q_{L,n}\left(\frac{t}{\varepsilon^2}\right)=\frac{-1}{2i\pi}\oint_{\gamma_u}\left(\frac{\tilde{b}}{a}\right)^*(z)z^{2n}\times\left(1-\frac{z^2e^{-ik+\mu}}{1-z^2e^{-ik-\mu}}\chi_\mu(x_s-n)\right)\times\left(1-\frac{1}{1-z^2e^{-ik-\mu}}\chi_\mu(x_s-n)\right)dz+\frac{\sinh^2(\mu)}{2i\pi}\frac{\exp(2ik(n-x_s)+2i\alpha_s)}{\cosh^2(\mu(n-x_s))}\times\oint_{\gamma_u}\frac{b}{a}(z)\frac{z^{-2n}e^{ik-\mu}}{(z^2-e^{ik-\mu})^2}dz, \tag{A9}$$

where $\chi_\mu(y)=e^{-\mu}\sinh(\mu)(1+\tanh(\mu y))$. q_S is the soliton part of the total wave. The first component of q_L represents the scattered wave packet, with a correction in the neighborhood of the soliton $n\sim x_s$. In front of the soliton $n\gg x_s$, the radiation is

$$q_{L,n}\simeq\frac{-1}{2i\pi}\oint_{\gamma_u}\left(\frac{\tilde{b}}{a}\right)^*(z)z^{2n}dz, \tag{A10}$$

while behind the soliton $n\ll x_s$ the radiation is

$$q_{L,n}\simeq\frac{-e^{-2\mu}}{2i\pi}\oint_{\gamma_u}\left(\frac{\tilde{b}}{a}\right)^*(z)z^{2n}\frac{(1-z^2e^{-ik+\mu})^2}{(1-z^2e^{-ik-\mu})^2}dz. \tag{A11}$$

The second component of q_L represents the interaction between the soliton and the scattered wave packet, which is only noticeable in the neighborhood of the soliton. This result is not surprising. Roughly speaking, the support of the scattered wave packet lies in an interval with length of order ε^{-2}. Since the l^2 norm is bounded by the conservation of the total mass, we can expect that the amplitude of the radiation is of order ε. More exactly, using the same arguments as in lemma 4.2 [8], it can be rigorously proved that the amplitude of the radiated wave packet can be bounded above by $K\varepsilon|\log\varepsilon|$.

(4) *Check a posteriori the adiabatic approximation*. The final part of the proof consists of checking *a posteriori* the adiabatic hypothesis, that is to say proving that the radiated wave packet determined here has no noticeable influence on the evolutions [Eqs. (53)] of the Jost coefficients a and b. One must estimate the components of the functions γ_1 and γ_2 given by Eqs. (57) and (58) which have been neglected until now, and which are related to the interplay between the soliton and the radiation, on the one hand, and which are due to the sole effect of the radiation on the other hand. These are technical calculations which are based upon the mixing properties of process V.

[1] P. Anderson, Phys. Rev. **109**, 1492 (1958).
[2] W. Kohler and G. Papanicolaou, J. Math. Phys. **14**, 1733 (1973); **15**, 2186 (1974).
[3] I. M. Lifshitz, S. A. Gredeskul, and L. A. Pastur, *Introduction to the Theory of Disordered Systems* (Wiley, New York, 1988).
[4] S. V. Manakov, S. Novikov, J. P. Pitaevskii, and V. E. Zakharov, *Theory of Solitons* (Consultants Bureau, New York, 1984).
[5] *Nonlinearity with Disorder*, edited by F. Kh. Abdullaev, A. R. Bishop, and St. Pnevmatikos (Springer, Berlin, 1991).
[6] Yu. S. Kivshar, S. A. Gredeskul, A. Sanchez, and L. Vasquez, Phys. Rev. Lett. **64**, 1693 (1990).
[7] V. A. Hopkins, J. Keat, G. D. Meegan, T. Zhang, and J. D. Maynard, Phys. Rev. Lett. **76**, 1102 (1996).
[8] J. Garnier, SIAM (Soc. Ind. Appl. Math.) J. Appl. Math. **58**, 1969 (1998).
[9] D. B. Mortimore and J. W. Arkwright, Appl. Opt. **29**, 1814 (1991).
[10] H. S. Eisenberg, Y. Silberberg, R. Morandotii, A. R. Boyd, and J. S. Aitchison, Phys. Rev. Lett. **81**, 3383 (1998).
[11] R. Hirota and J. Suzuki, J. Phys. Soc. Jpn. **28**, 1366 (1970).
[12] R. Hirota and J. Satsuma, J. Phys. Soc. Jpn. **40**, 891 (1976).
[13] N. Mott, *Conduction in Non-Crystalline Materials* (Oxford University Press, Oxford, 1987).
[14] A. B. Aceves, C. De Angelis, T. Peschel, R. Muschall, F. Lederer, S. Trillo, and S. Wabnitz, Phys. Rev. E **53**, 1172 (1996).
[15] M. J. Ablowitz and J. F. Ladik, Stud. Appl. Math. **55**, 213 (1976).
[16] R. Scharf and A. R. Bishop, Phys. Rev. A **43**, 6535 (1991).
[17] Ch. Claude, Yu. S. Kivshar, O. Kluth, and K. H. Spatschek, Phys. Rev. B **47**, 14 228 (1993).
[18] Yu. S. Kivshar and D. K. Campbell Phys. Rev. E **48**, 3077 (1993).
[19] M. J. Ablowitz and J. F. Ladik, J. Math. Phys. **16**, 598 (1975).
[20] L. D. Faddeev and L. A. Takhtajan, *Hamiltonian Methods in the Theory of Solitons* (Springer-Verlag, Berlin, 1987).
[21] M. J. Ablowitz and J. F. Ladik, J. Math. Phys. **17**, 1011 (1976).
[22] D. Middleton, *Introduction to Statistical Communication Theory* (McGraw Hill, New York, 1960).
[23] A. A. Vakhnenko and Y. B. Gaididei, Theor. Math. Phys. **68**, 873 (1986).
[24] L. Arnold, G. Papanicolaou, and V. Wihstutz, SIAM (Soc. Ind. Appl. Math.) J. Appl. Math. **46**, 427 (1986).
[25] G. Dahlquist and A. Björk, *Numerical Methods* (Prentice-Hall, Englewood Cliffs, NJ, 1974).